

MICROSCOPE – fabricating test masses for an in-orbit test of the equivalence principle

Daniel Hagedorn^{1,*}, Heinz-Peter Heyne¹, Stephan Metschke¹, Uwe Langner¹, Sven Grüner¹, Frank Löffler¹, Vincent Lebat², Manuel Rodrigues², and Pierre Touboul³

Received 25 March 2013, revised 21 May 2013, accepted 24 June 2013
Published online 23 July 2013

The MICROSCOPE space mission is to test in 2016 the Weak Equivalence Principle (WEP) with an accuracy of 10^{-15} . This fundamental physics mission should provide answers to the basic question of the universality of free-falling bodies in a uniform gravity field. During 18 months, the mission should improve the current ground experiments by at least two orders of magnitude. The payload is composed of two electrostatic differential space accelerometers that exhibit a resolution of $2 \times 10^{-12} \text{ m s}^{-2} \text{ Hz}^{-1/2}$. By measuring the difference of acceleration between two concentric test masses at the orbital frequency, a possible WEP violation signal is extracted from the measurement where the gravity gradient effect dominates by a factor of one hundred.

This paper addresses the scientific objective of the space mission and describes how the performance drives the specification. A particular focus is made on the work jointly performed by ONERA and PTB to fulfil the fabricating requirements.

1 The weak equivalence principle test motivation

The WEP states that gravity acts on all bodies placed in a uniform gravitational field in the same way and that the acceleration is independent of the mass or composition of the body. In other words, acceleration cannot be distinguished from gravity for “free-falling objects”. On this principle, Einstein founded the gravitation theory, i.e. General Relativity.

Nevertheless, some theoretical developments [1] point to a possible range of EP violation [10^{-14} – 10^{-21}] as a consequence of the coupling between matter and the string dilaton, one of the promising candidates for an alternative theory of gravitation. A test of 10^{-15} , as foreseen

for MICROSCOPE, is of major interest to differentiate between the alternative candidates.

To achieve this challenge, the geometry of the core parts of the accelerometers, i.e. the electrodes and the test masses, must be machined with an accuracy of a few micrometers in order to guarantee the fine electrostatic operation of the instrument and a maximum in-orbit test-mass centering displacement of $20 \mu\text{m}$. With the help of the in-orbit calibration process, the test-mass centering is afterwards computed with $0.1 \mu\text{m}$ accuracy in order to subtract the effect of the Earth’s gravity, which is a well-known gradient from the acceleration data. Thus, the performance of the mission relies dramatically on the machining and precise metrology of the parts of the sensor core and particularly on the test masses.

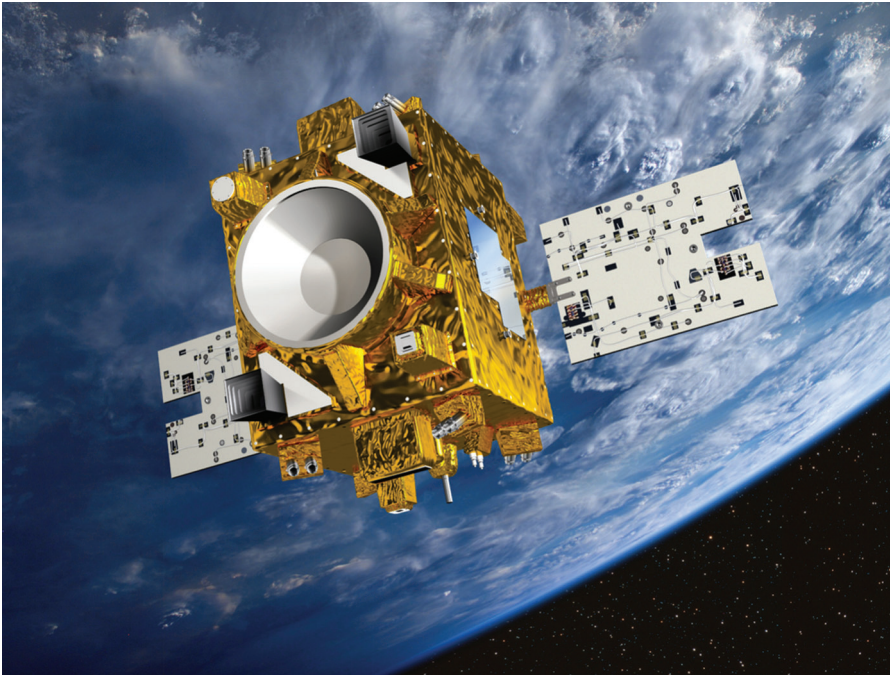
In the best ground test [2] a torsion pendulum was operated by the EötWash group. Test masses made of copper, aluminum, silica, titanium or beryllium were used. To cope with perturbation signals in the laboratory, the authors placed the test masses on turntables in order to modulate the signal to a higher frequency, helping also to reject part of the long-term drift or of the stochastic errors. The best achieved accuracy of this experiment is $(0.3 \pm 1.8) \times 10^{-13}$ with Be and Ti test masses. Besides statistical errors, the main source of disturbance originates in time variations of gravity gradients and thermal noise. For the former, it depends mainly on the environment: seismic and human activities, building stability, gravity gradients from nearby hills, etc. Optimistic

* Corresponding author E-mails: daniel.hagedorn@ptb.de

¹ Physikalisch-Technische Bundesanstalt (PTB), Bundesallee 100 D-38116, Braunschweig, Germany

² Office National d’Etudes et de Recherches Aérospatiales (ONERA), 29 avenue de la Division Leclerc 92320, Châtillon, France

³ ONERA, Chemin de la Hunière, BP 80100, 91123 PALAISEAU CEDEX Palaiseau, France



© CNES - Juillet 2012 / Illust. D. Ducros

Figure 1 An artist's view of the MICROSCOPE satellite (courtesy of CNES).

projections for improving the sensitivity suggest one order of magnitude within 5 years.

2 The MICROSCOPE mission and performance drivers

The MICROSCOPE (Micro-Satellite à traînée Compensée pour l'Observation du Principe d'Equivalence) mission is a European space fundamental physics experiment led by the French Space Agency, CNES, with a satellite launch in 2016, see illustration in Fig. 1. Proposed by the Observatoire de la Côte d'Azur and ONERA [3] in the frame of the CNES Myriad microsatellite programme, MICROSCOPE takes advantage of the best technologies currently available to perform the WEP test in space with an accuracy of at least 10^{-15} [4]. Performing the WEP test in space allows limiting all gravitational disturbances due to seismic noise or human activity. The residual gravity disturbance remaining due to the satellite thermal expansion has been estimated to be less than $2 \cdot 10^{-16} \text{ m s}^{-2}$ and is thus compatible with the mission objectives. Moreover, one can take advantage of long measurement periods with the 18-month mission leading to about 1200 useful orbits for the benefit of the rejection of stochastic disturbances.

At the core of the MICROSCOPE satellite, the payload is composed of two differential electrostatic space ac-

celerometers, see Fig. 2. Each of the accelerometers contains one pair of test masses. The first instrument serves to test the WEP (outer test mass TiAl6V4, inner test mass PtRh10), while results from the second one (both PtRh10) are to help to eliminate systematic errors as no violation signal is obviously expected for the same material.

3 Measurement equation and performance objective

For an ideal test of the EP one would use two spherical test masses with identical radii and a perfectly homogeneous density distribution located at the same point. As such, a configuration cannot be realized in an actual experimental setup, test masses in the form of hollow cylinders have been selected. For technical reasons, additional features are required as described below. However, the shape has been optimized to obtain the same value of the inertia matrix along the three axes, as is the case for the sphere. Indeed, a difference of inertia values induces a defect in the angular measurement output of the accelerometer that does not purely depend on angular acceleration.

In the MICROSCOPE project, in each accelerometer, two hollow cylinders, aligned as concentrically as possible, are orbiting in the Earth's gravity field.

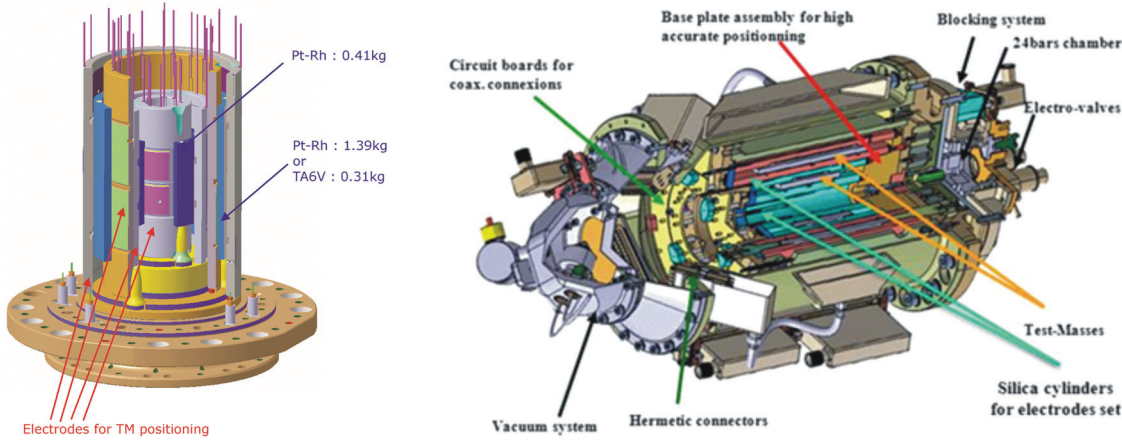


Figure 2 Left: Test masses surrounded by the electrodes. Right: Cut-off of the sensor unit with its sensor core, the blocking mechanism for in-orbit test-mass release, the vacuum system.

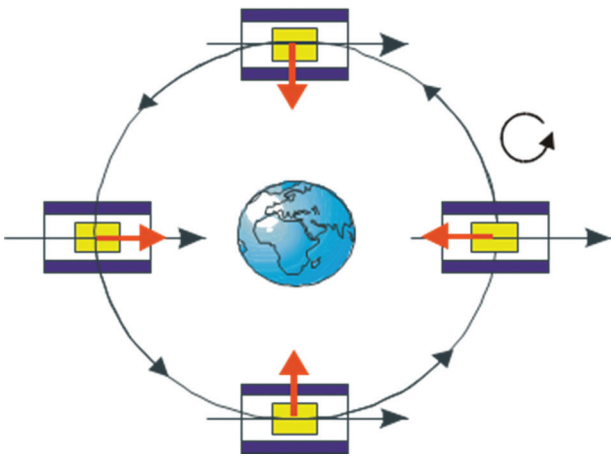


Figure 3 Orbital motion of MICROSCOPE: measurement frame in black, gravitational field in red.

Electrostatic fields maintain both test masses motionlessly with respect to the surrounding sensing electrodes. By finely measuring the difference of the electrostatic forces needed to maintain the two bodies in a motionless state, one can deduce whether both test masses are being accelerated equivalently or not. To take advantage of the accelerometer performance, the satellite is maintained in an inertial pointing mode or slowly rotated about the axis normal to the orbital plane, see Fig. 3. The Earth's gravity field is then projected either along the measurement axis at the orbital frequency or at the satellite rotation frequency in addition to the orbital frequency. More details of the satellite and the instrument description are provided in ref.4.

The requirements concerning the accuracy of the test-mass geometry can be deduced as follows. In a per-

fect free fall, the test-mass acceleration is expressed by Newton's law:

$$m_{Ik} \overrightarrow{\Gamma_{App,k}} = m_{Gk} \vec{g}(O_k),$$

where m_{Ik} is the inertial mass of the body placed in O_k and $\overrightarrow{\Gamma_{App,k}}$ is its acceleration.

In a uniform gravity field, the force exerted on the mass is $m_{Gk} \vec{g}(O_k)$, g expressing the gravity field and m_{Gk} the gravitational mass of the body. The WEP implies: $m_{Ik} = m_{Gk}$ and $\overrightarrow{\Gamma_{App,k}} = \vec{g}(O_k)$.

In the MICROSCOPE experiment, the test masses are submitted to electrostatic forces \vec{F}_{el_k} which maintain the bodies motionlessly with respect to the satellite that in turn is submitted to nongravitational forces (drag, radiation pressure) \vec{F}_{ext} and to thruster actuations \vec{F}_{th} . O_{sat} describes the center of gravity of the satellite.

The applied acceleration to the mass k in the test-mass reference frame is expressed by:

$$\overrightarrow{\Gamma_{App,k}} = \frac{\vec{F}_{el_k}}{m_{Ik}} = \frac{M_{Gsat}}{M_{Isat}} \vec{g}(O_{sat}) - (1 + \delta_k) \vec{g}(O_k) + R_{In,COR}(\overrightarrow{O_{sat}O_k}) - \frac{\vec{F}_{pa_k}}{m_{Ik}} + \frac{\vec{F}_{ext}}{M_{sat}} + \frac{\vec{F}_{th}}{M_{Isat}}.$$

The term $\frac{\vec{F}_{pa_k}}{m_{Ik}}$ expresses the contribution of the internal parasitic forces applied to each mass k .

The term $\frac{m_{Gk}}{m_{Ik}} = 1 + \delta_k$ expresses the ratio of the gravitational mass to the inertial mass, which is different from unity if the EP is violated and depending on the test-mass material [1]. The gravitational mass M_{Gsat} and the inertial mass M_{Isat} of the satellite are also considered.

The term $R_{In,COR}(\overrightarrow{O_{sat}O_k})$ stands for the inertia and the Coriolis accelerations in the satellite frame due to

the satellite attitude motion. If the test-mass electrostatic control is sufficiently stiff, the residual relative motion can be neglected and the inertia effect is simply expressed by: $\vec{\Omega} \wedge \overrightarrow{O_{\text{sat}} O_k} + \vec{\Omega} \wedge (\vec{\Omega} \wedge \overrightarrow{O_{\text{sat}} O_k})$, where $\vec{\Omega}$ represents the angular velocities of the satellite with respect to the inertial reference frame.

Finally, the expression of the differential acceleration applied on the two test bodies (*i*) and (*j*) is given by:

$$\begin{aligned} \overrightarrow{\Gamma_{\text{App},i}} - \overrightarrow{\Gamma_{\text{App},j}} &= (\delta_j - \delta_i) \vec{g}(O_j) + (1 + \delta_i) [T] \overrightarrow{O_i O_j} \\ &\quad - R_{\text{In,COR}} \left(\overrightarrow{O_i O_j} \right) - \frac{\vec{F} p a_i}{m_{i i}} + \frac{\vec{F} p a_j}{m_{j j}} \\ &= \overrightarrow{\Gamma_{\text{app},i}} - \overrightarrow{\Gamma_{\text{app},j}} - \frac{\vec{F} p a_i}{m_{i i}} + \frac{\vec{F} p a_j}{m_{j j}} \end{aligned}$$

$O_i O_j$ is the distance between the two bodies.

$[T]$ is a linear approximation of the gravity field variations:

$$\vec{g}(O_j) - \vec{g}(O_i) = [T] \overrightarrow{O_i O_j} + O(T^2).$$

The second-order gravity development terms T^2 are very small indeed, leading to an acceleration residual smaller than $2 \times 10^{-17} \text{ m s}^{-2}$.

$(\delta_j - \delta_i) \vec{g}(O_j)$ represents the violation signal of the EP if it exists.

At the 700 km-altitude of the microsatellite, the Earth's gravity has a value of 7.96 m s^{-2} . In order to detect a potential EP violation at 10^{-15} , it is necessary to measure a difference of acceleration as small as $(\delta_j - \delta_i) \vec{g}(O_j) = 7.96 \times 10^{-15} \text{ m s}^{-2}$ at the EP test frequency. This is the objective of accuracy of the differential accelerometer: all sources of error are evaluated and their contributions to the global accuracy are summarized hereafter [4].

4 Centering requirements

$$(1 + \delta_i) [T] \overrightarrow{O_i O_j} \approx [T] \overrightarrow{O_i O_j}$$

represents the effect of the Earth's gravity gradient, because the test-mass alignment cannot be perfectly concentric. The components of $[T]$ have amplitudes of less than $5 \times 10^{-9} \text{ m s}^{-2}/\text{m}$ at the measurement frequency (i.e. the orbital frequency with an inertial pointing satellite). Hence, the test-mass centering accuracy must be specified to $0.1 \mu\text{m}$ along the two directions of the orbital plane that are affected by the Earth's monopole term. This specification cannot be achieved with any technology available.

Fortunately, the Earth's gravity is very well known, an achievement of the space missions GRACE and GOCE [5]. By evaluating the effect of the Earth's gravity gradient at twice the orbital frequency, the off-centering is calibrated in the orbital plane and its effect at orbital frequency can thus be subtracted.

The application of this in-orbit procedure [4] allows the relaxation of the requirement of the test-mass centering during integration to $20 \mu\text{m}$. This specification must include the following error contributors:

- the electrostatic biasing;
- the machining limitations; and
- the accuracy of the mounting process (integration).

The former is due to electronics offsets of the position sensor that are wrongly interpreted by the servoloop accelerometer as a test-mass displacement. This contribution is easily measured on the ground through the electronics characterisation and has been optimized in terms of value and stability, its overall contribution being less than $0.2 \mu\text{m}$.

The second contributor to the off-centering is caused by deviations from the optimal geometry of the sensor core that modifies the electrostatic field between the sensor electrodes made of gold-coated silica and the test masses. The silica parts are obtained by a specific ultrasonic machining process that allows an accuracy of a few micrometers when assisted by laser interferometry as in situ control.

As shown in Fig. 4, the operation of the electrostatic loop will move the mass according to the defects of symmetry of the geometry. When the test mass moves towards the right, the capacitance on the right, C_2 , increases while the capacitance on the left, C_1 , decreases. If the geometry were ideal, C_1 would equal C_2 when the test mass was centered. The electrostatic servo loop acts to equalise the two capacitances and thus the test mass remains motionless and centered in the electrode frame (along X in this simple example). If the test mass is shaped as a cone of angle α , the servo loop will again displace the test mass in order to equalise both capacitances. But due to the small slope, C_1 and C_2 are not symmetric and the test mass is displaced by δl evaluated in this case to:

$$C_1 = C_2 \quad \text{when} \quad x = \delta l = -\alpha \frac{(L_{\text{PM}} - L_{\text{el}}) L_{\text{el}}}{2 \text{gap}}.$$

For the qualification test-mass model, the angle is about $7 \mu\text{m}$ over the 60-mm length leading to a generated miscentering of $30 \mu\text{m}$. To cope with this value, which is too large, the defects on the electrode cylinders, when smartly orientated, can compensate the

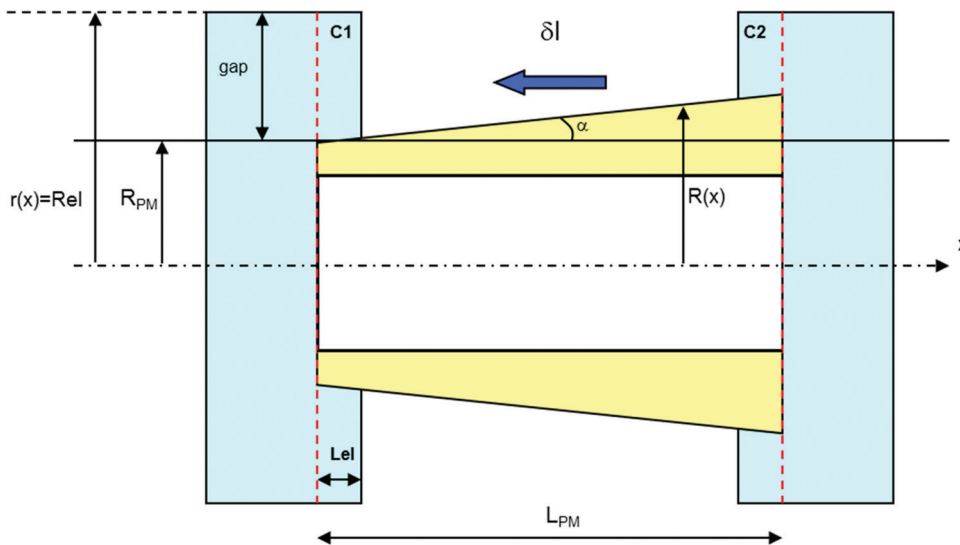


Figure 4 Schema of a TM conicity for the capacitance sensing position of the test-mass TM along X.

test-mass defects: fortunately this was the case. For the flight models, the machining procedures have been optimized and this defect has been reduced by one order of magnitude.

For the third contributor, the relative centering of the two concentric test masses relies also on the mounting procedure of the overall core that accurate machining and permanent metrology enable to guarantee an accuracy of a few micrometers.

5 Acceleration disturbances in the measurement

$-\frac{\vec{F} p a_i}{m_i} + \frac{\vec{F} p a_j}{m_j}$ represents the difference of the parasitic acceleration applied on the two test masses: stochastic accelerations and systematic tone errors at the EP measurement frequency must be considered.

As the orbital motion can be maintained very stably because of the drag-free satellite, one can take advantage of very long steady periods of integration in order to reduce the stochastic noises to a level of a few $10^{-15} \text{ m s}^{-2}$. The instrument's major source of noise, the mechanical residual damping of the test mass, is of the order of $2 \times 10^{-12} \text{ m s}^{-2} \text{ Hz}^{-1/2}$. Integrating over 120 orbits ($\sim 7 \times 10^5 \text{ s}$) reduces this contribution to $2.4 \times 10^{-15} \text{ m s}^{-2}$ at the EP measurement frequency.

$R_{\text{in,COR}}(\overrightarrow{O_{\text{sat}} O_k})$ represents the effect of the satellite angular velocity or angular acceleration. This term can only be controlled by the satellite attitude system [4]. The accelerations along the 6 degrees of freedom are fortunately provided by the instrument itself, and the satellite-

pointing system nullifies the angular acceleration measured by the 6-axis accelerometers. Nevertheless, the angular and linear axes of the measurement depend on the test-mass shape and inertia. Thus, the requirements of the test-mass geometry are deduced.

6 Developing the test masses: test mass description

Each hollow cylinder test mass for the MICROSCOPE differential accelerometer has four flat areas at the outer shell and six precision countersinks at each face. The flat areas are used to control the test-mass rotation, while the countersinks serve as seats for the blocking mechanism that clamps the test masses during launch.

The large PtRh10 and TiAl6V4 test masses are 69.395 mm in outer diameter, 60.800 mm in inner diameter, and have a length of 79.830 mm – tolerance: $3 \mu\text{m}$ and below. The small PtRh10 test masses are 34.400 mm in outer diameter, 30.800 mm in inner diameter, and have a length of 43.332 mm – tolerance: $3 \mu\text{m}$ and below.

TiAl6V4 is used in aeronautics and motorsports due to its machinability and form stability in the range of less than $10 \mu\text{m}$. However, to achieve and maintain form and dimension tolerances of less than $5 \mu\text{m}$, a multi-stage heat treatment and special low-force turning parameters have to be applied. PtRh10 is a soft and ductile material and therefore not ideal for turning. Only a small window of cutting parameter space (turning speed, feed, amount of lubricant sprayed at the tool) and the use of polycrystalline diamonds lead to an acceptable surface quality.

However, because of the overall geometrical complexity of the test masses with stringent requirements on shape, sizes and center of gravity, and due to the fact that each surface is referenced to all connecting surfaces, turning is the technology of choice for the manufacturing of all test masses [6].

7 Developing the test masses: the need for high-precision in situ measurement

Any form of mechanical machining is subject to tool wear. In standard applications a mean time before tool wear-out or failure is determined, by which time the tool has to be replaced. In the case of the fabrication of the MICROSCOPE test masses, this approach is not applicable, because even small defects or extraordinary wear of the cutting tool due to surface anomalies like hard rhodium clusters embedded in softer platinum surroundings may lead to a significant form deviation or even damage to the test-mass surface beyond any repair. This is, of course, especially valid at the end of the fabrication, when all dimension, form and surface roughness parameters have to be achieved with one last and final cut.

In order to gain the information necessary for the correction and, of course, the determination of the final form and dimensions, high-precision in situ measuring equipment has to be installed inside the BENZINGER *TNI* precision fabrication station. As the fabrication tools use the same frame as the measuring equipment, two distinct adjustment steps are necessary.

First, certified ring and plug gauges (the outer and inner diameters of which, respectively, are identical to those of the final test masses and whose cylindricity is within the specifications of the test masses, as well) are placed at the exact position the test mass will be mounted at during fabrication. The diameter is determined by contact measurement (using a Renishaw OMP 400 high accuracy touch probe and SiN balls to minimise adhesion) of several tens of points along the respective diameter and calculating the best fitting circle and its respective diameter. The in situ measurement verification of the inner and outer diameter has to pass a rigorous regime of measurement and repetition measurement. Only if the comparison of all measurements shows a deviation of less than one micrometer, is the adjustment regarded as successful.

Secondly, during test-mass fabrication, along several z -axis positions (the z -axis being the central axis of the adjustment standard/test mass), the inner and outer di-

ameters are measured. Additionally, the distance from the test-mass center, the flatness and the angle of all four flats of the body are measured, too. Hereafter, the adjustment standard is transferred to a coordinate measuring machine (CMM) and measured against calibrated gauges at exactly the same positions. The results are in turn used to adjust the precision fabrication machine. The overall uncertainty budget has been verified to be less than two micrometers. Results above this limit are rejected and the procedures are repeated in total.

Through this approach, the results are traceable to the SI unit of length.

Only the combination of both adjustment procedures guarantees reproducible results. The second step is vital to the success, because both the tool holder and the measuring setup are mounted at the same frame. Thus, defects of the frame itself cannot be detected using the first method only.

Though it may seem that other methods of mechanical engineering like polishing or even electrical discharge machining (EDM) might be advantageous over turning, this is only true for single aspects of the overall fabrication work flow. Polishing, for example, would result in an improved surface roughness, especially of the PtRh10 alloy. Still, other parameters like concentricity or precision of angles with its very low tolerances could not be achieved. Not least the position and depth of the countersinks, especially on the second face, call for an exact knowledge of both the test mass and the tool positions. At a precision fabrication station, the whole manufacturing of the test mass can be achieved in just two clamping positions.

Upon beginning the fabrication, a thread is cut at one end of the hollow cylinder and the raw-mass is screwed against the dead stop of a custom-made brass adapter. In this way the mounting forces are directed almost completely in the z -direction and any unloading of stress after unmounting the finished test mass is reduced to the technical minimum, see Fig. 5.

Whilst clamping the first face, the inner and outer diameter, the four flats at the outer shell, the 45° angle chamfers connecting the faces and the inner and outer shell along with the six countersinks are fabricated. The form and aperture of the countersinks are determined by carefully selecting optimal styli, test drilling countersinks using identical materials and drilling parameters, measuring the test countersinks on a specialized CMM (ZEISS F25), and, additionally, allowing for tool wear.

Hereafter, the test mass is unmounted and the thread is removed by means of wire EDM. Then, the test mass is mounted at the precision fabrication station again, this time using an adapted clamping system (Hainbuch

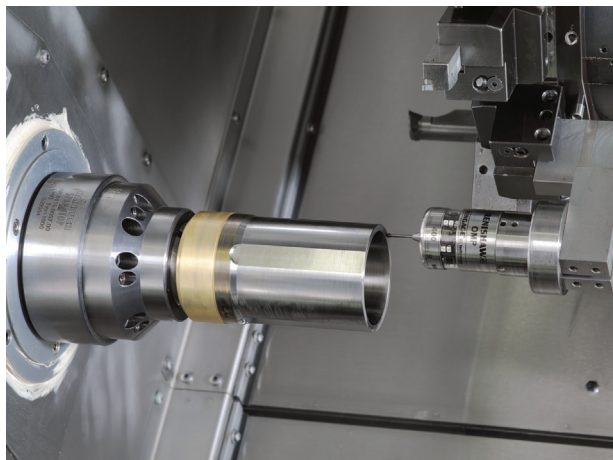


Figure 5 PtRh10 TM mounted at a brass adapter and testing probe inside the precision fabrication station.



Figure 6 One large Ti TM fixed at the measuring stand at the Leitz reference 600 CMM.

company), which allows secure clamping, while at the same time not damaging the inner shell's surface.

Once again, the motion control system of the precision fabrication station is adjusted against a calibrated gauge block and then the length, the second face, and the final six countersinks are fabricated.

8 Developing the test masses: measuring the test masses

After fabrication, the test masses undergo extensive measurements. Besides form and dimension measurements [7], density, thermal expansion, and the mass are determined also.

The form and dimension measurements consist of tactile measurements performed using a calibrated Leitz reference 600 CMM, see Fig. 6. Basically, for reasons of comparability, measurements are performed at exactly the same positions as they were conducted during fabrication with respect to circumference and the z -axis. To gain a higher resolution, additional measurements were taken between these points and at additional z -positions especially close to the faces. From these results, all necessary features (diameters, length, concentricity, parallelism, planarity of both the flats and the faces, position of countersinks) are determined. Figure 7 shows a photo composition of the inner and the outer test mass.

Tactile measurement has been chosen, since the accuracy of optical methods was found to be inadequate as a result of the roughness of the test-mass surfaces. While for the Ti alloy a surface roughness of about $R_a \approx 100$ nm was achieved, which would allow the use of optical meth-

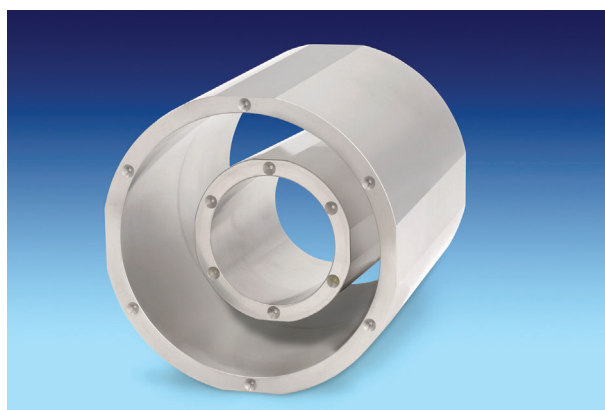


Figure 7 Photo composition of both inner and outer TM.

ods, the surface roughness of the PtRh10 was found to be about a factor of three higher, leading to a significantly larger error budget, when optical measurements were conducted during the development of the fabrication and measuring procedure.

As a rule, before and after the measurement of the test masses, custom-made calibrated gauges with diameters identical to those of the test masses are measured. Then each test mass is measured in four positions: horizontally mounted, inverse horizontally mounted, vertically mounted, and inverse vertically mounted. All measurement results have to comply with the two-micrometer criterion of the overall uncertainty budget.

The countersinks are measured using the ultraprecision CMM ZEISS F25. Here, position, depth, aperture, and the angle of the countersink's central axis with respect to the faces are determined.

All additional measurements (density, thermal expansion, and mass) are performed by PTB's dedicated laboratories.

The density of the test masses is determined by direct measurement of all test masses, apart from the large PtRh10 mass, because it is too heavy for the setup available. An uncertainty of up to 5×10^{-5} can be reached.

A direct measurement of the density distribution to determine the test-masses' multipole moments was considered, but finally rejected due to insufficient resolution. Instead, in addition to the density measurement of the test mass itself, the density of rings, separated from both ends of the test masses, were measured and the respective results were compared. It was found that, in all cases, the measured density was in a band of 1×10^{-4} and, hence, the density distribution was regarded as adequate.

The thermal expansion coefficient is measured in the range from 18 °C to 24 °C with an uncertainty of 10^{-8} . As the space experiment is conducted at about 300 K, this is the range of choice.

Finally, the mass is determined with a precision of below 10^{-7} .

9 Conclusion and outlook

The MICROSCOPE space test of the Weak Equivalence Principle will be launched in 2016 on board a drag-free satellite. The experiment will operate on a polar orbit for about two years. The two differential accelerometers at the core of the experiment each hold two test masses comprising PtRh10 and TiAl6V4 alloys.

The 10^{-15} accuracy of the test, the electrostatic operation of the instrument, the capacitive position sensing of the test masses, as well as the corrections of the mass off-centering, require a demanding geometry. Extensive effort has been carried out to develop the means for both fabrication and measurement of the necessary core components, foremost the silica casing and the test masses. A fabrication precision has been achieved, formerly unreachable for these kinds of materials, guaranteeing the necessary in-orbit centering accuracy of 20 μm . The flight models of the test masses were produced according to the precisions established and meet the mission requirements.

Though the experiment is not completed at the time of writing, the community is already discussing a follow-up mission. Several concepts are on the table, not least the development of an orbit-based, superconducting accelerometer, which could improve the experiment's uncertainty down to the 10^{-18} range, but with even more stringent requirements on the test masses.

Acknowledgements. PTB's Scientific Instrumentation Department would like to thank the dedicated PTB Departments of Mass (1.1), Analytics and Thermodynamic State Behaviour of Gases (3.2), Dimensional Nanometrology (5.2), Coordinate Metrology (5.3), and Interferometry on Material Measures (5.4) for their valuable support in metrological characterisation of the test masses. The authors also want to acknowledge the CNES for their support and funding to develop the payload, the national aeronautics and space research center of the Federal Republic of Germany (DLR) for supporting the test-mass material, the Bremen ZARM centrum for their contribution to the qualification and acceptance tests of the payload in free-fall conditions. Part of the work is funded by ONERA and PTB.

Key words. fundamental physics, equivalence principle, space mission, precision engineering, in-line measurement.

References

- [1] T. Damour and A. M. Polyakov, Nucl. Phys. B **423/3–2** 855–235 (1994).
- [2] S. Schlamminger, K.-Y. Choi, T. A. Wagner, J. H. Gundlach, and E. G. Adelberger, Phys. Rev. Lett. **100**, 041101 (2008).
- [3] P. Touboul, M. Rodrigues, G. Métris, and B. Tatry, Comptes Rendus de l'Académie des sciences, IV-tome 2-N, 9 (2001).
- [4] P. Touboul, G. Métris, V. Lebat, and A. Robert, Class. Quantum Gravity **29** (2012).
- [5] P. Touboul, B. Foulon, M. Rodrigues, and J. P. Marque; Aerospace Sci. Technol. **8**, 431–441 (2004).
- [6] D. Hagedorn, H.-P. Heyne, H. Reimann, M. Neugebauer, S. Grüner, St. Metschke, and F. Löffler, ISBN **13**: 978-0-9553082-6-0, 29-32, EUSPEN 2009.
- [7] O. Jusko, N. Gerwien, D. Hagedorn, F. Härtig, H.-P. Heyne, U. Langner, F. Löffler, St. Metschke, M. Neugebauer, and H. Reimann, Proc. ISPEMI 2010, 6th International Symposium on Precision Engineering Measurements and Instrumentation, 8.-11.8. 2010, Hangzhou, China.